TELKOMNIKA, Vol.17, No.5, October 2019, pp.2169~2178
ISSN: 1693-6930, accredited First Grade by Kemenristekdikti, Decree No: 21/E/KPT/2018
DOI: 10.12928/TELKOMNIKA.v17i5.12803

Full-duplex user-centric communication using non-orthogonal multiple access

Sock Theng Ooi*[1], Razali Ngah[2], Marwan Hadri Azmi[3]
Wireless Communication Centre, School of Electrical Engineering,
Faculty of Engineering, Universiti Teknologi Malaysia, Malaysia
*Corresponding author, e-mail: sockthenng81@gmail.com[1], razalin@fke.utm.my[2], hadri@fke.utm.my[3]

Abstract

This paper proposes an improved user-centric Non-Orthogonal Multiple Access (NOMA) communication in two-base station networks with in-band full duplex (IBFD) user. We derive the achievable rates of the proposed user-centric NOMA systems. For benchmarking purposes, we also derive the achievable rate for the user-centric system deploying conventional NOMA schemes, Orthogonal Multiple Access (OMA) schemes and point-point communication systems. We then analyze and simulate the performance of the proposed and all the benchmarked systems. We found that our proposed user-centric NOMA approach has a 64% improvement in the total achievable rate when compared to the benchmarked approach under similar power constraint.

Keywords*: achievable rates, in-band fullduplex (IBFD), non-orthogonal multiple access (NOMA), successive interference cancellation (SIC), user-centric network (UCN)*

1. Introduction

Over the last few years, wireless terminals are equipped with a more advanced function as transmitter and receiver, e.g., base stations, relays, or mobiles, due the advancement of the modern wireless communication systems [1]. With these unique and advanced features possess by the wireless terminals, it drives the quest for the use of in-band full duplex (IBFD) wireless transceivers. Conventionally, the terminal operates using half-duplex modes, where it can only transmit or receive at one time. Therefore, with the IBFD, the wireless terminals are able to transmit and receive simultaneously over the same frequency band. This new full-duplex capability provides a promising potential that can lead to a two-fold spectral efficiency gain [2].

The fifth generation (5G) mobile system is expected to be deployed widely in the near future [3]. Stronger multiple access (MA) schemes have been identified as one of the key techniques to support large-scale heterogeneous traffic and users in the upcoming 5G systems. In recent years, non-orthogonal multiple access (NOMA) have gained a lot of research interest due to its promising capabilities to achieve higher spectrum efficiency, and to support massive connectivity [4-13]. Unlike the conventional multiple access that are based on the orthogonality of the resources in either time, code or frequency domains (i.e. TDMA, CDMA, OFDMA), NOMA has been shown to accommodate more users by allocating them on the non-orthogonal resource, which consequently attain high spectrally efficient radio access and network capacity [14-16]. Power domain (PD) NOMA schemes result in non-orthogonality among users, where multiple users share the same frequency resources simultaneously by utilizing superposition coding at the transmitter and successive interference cancellation (SIC) at the receiver [17, 18]. Although NOMA has recognized as a promising multiple access technique for 5G but most of the researchers have focused on downlink traffic only [19, 20]. Uplink traffic begins to attract the attention since the emergence of new mobile and Internet-of-Things (IoT) applications. Uplink traffic plays a significant role when the IoT experiences massive growth, which incur intensive uplink traffic by sensing and monitoring characteristic [21].

Apart from a more advanced IBFD capability and stronger MA schemes, user-centric network (UCN) has also been identified to become new key enabler for 5G networks to provide ubiquitous high-speed connectivity to mobile users. Traditional cell-centric networks construct the network, where each handset communicates with only one specific cell site at a time. Under UCN architecture, multiple cell sites that located around the mobile user are cooperating to

Received October 30, 2018; Revised April 3, 2019; Accepted May 1, 2019

provide high data rates to the users in every transmission, letting the mobile user to experience like the networks is always following it. Furthermore, UCN could intelligently recognize the mobile user's wireless communication and then can flexibly organize the required cell group and resource to serve the mobile users [22-25]. In [20], a local anchor based dual connectivity is proposed for UCN as it showed that the average user spectrum efficiency achieves an increase of 5% gains over the current LTE system while providing seamless coverage and borderless service to a mobile user. In another set of works, there are also studies in both traffics using coordinating multiple points (CoMP) approach with IBFD in 5G [1, 24].

Motivated by the challenging requirements of 5G systems to provide high-speed connectivity, this paper proposes a new user-centric NOMA communication in two-base station networks with IBFD user. The achievable rates of the proposed system are derived. We then analyze and simulate the performance of the system, and compared it with the performances of state-of-the art orthogonal multiple access (OMA) and point-point communication systems. The rest of the paper is organized as follows. In section 2, we present the system model for the proposed user-centric NOMA scheme and all benchmarked systems. Section 3 then derives the theoretical achievable rate for all studied and benchmarked schemes in this work. Section 4 presents and discusses the simulation results in terms of the achievable rate attained by all schemes. Finally, the conclusions are presented in section 5.

2. System Model

Consider a user centric architecture in which two base stations, BS_i for i∈{1,2,u} are supporting a user cooperatively using non-orthogonal multiple access (NOMA) schemes. Each base station has it owns independent messages to be forwarded to the user. The studied network topology consisting these three nodes is illustrated in Figure 1, where the distance between the two base stations is normalized to one. The user is located in a straight line between the two base stations with the distance of d_1 from BS_1. All the nodes in the considered scenario are equipped with a single antenna. The channel modeling used in this paper is described as follows. The channel gain between node i and node j is modeled as $\gamma_{ij} = \frac{1}{L_{ij}}$, where $L_{ij} = d_{ij}^{\alpha}$ denotes the path loss, d_{ij} is the distance between node *i* and node *j*, and α is the path loss exponent parameter. Using subscripts 1, 2 and u to denote the BS_1, BS_2 and the user node, respectively, the channel gains for all the links in Figure 1 are $\gamma_{1u} = \gamma_{u1} = \frac{1}{{d_{1u}}^{\alpha}} = \frac{1}{{d_{u1}}^{\alpha}}, \gamma_{12} = \gamma_{21} = 1, \gamma_{2u} = \gamma_{u2} = \frac{1}{{d_{2u}}^{\alpha}} = \frac{1}{{d_{u2}}^{\alpha}}$.

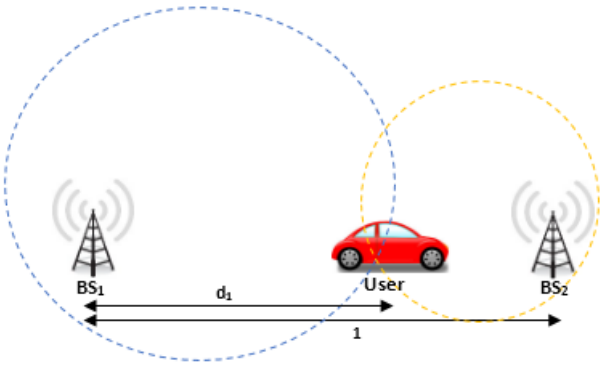

Figure 1. Effects of selecting different switching under dynamic condition

In this work, two NOMA schemes are developed, named case 1 and case 2 schemes. Case 1 is the conventional NOMA schemes that consist of mode A and mode B, as in Figure 2. Mode A is a downlink transmission whereby the user receives two distinct messages from both base stations during first time slot. Mode B is the uplink transmission, which occurs in the second time slot to concurrently forward distinct messages from user to both base stations.

Denoting the transmitted signal from node i as X_i and the received signal at node j as Y_j, the received signals for Case 1 are defined as:

$$Y_U = h_{1u}X_1 + h_{2u}X_2 + N_o \quad (1a)$$

for mode A and

$$Y_1 = h_{u1}(X_1 + X_{2)} + N_o \quad (1b)$$

$$Y_2 = h_{u2}(X_1 + X_{2)} + N_o \quad (1c)$$

for mode B. Here h_{ij} is the channel realization from node i to node j, while N_o is the noise realizations at the respective receivers. The noise is Gaussian with zero mean and unit variance, N_o~ N(0,1). We consider static-one dimensional additive white Gaussian noise (AWGN); however, extension to circularly symmetric AWGN channels is straightforward. Perfect global channel knowledge is assumed at all nodes. In this paper, the transmit power at each node i is set to P_i.

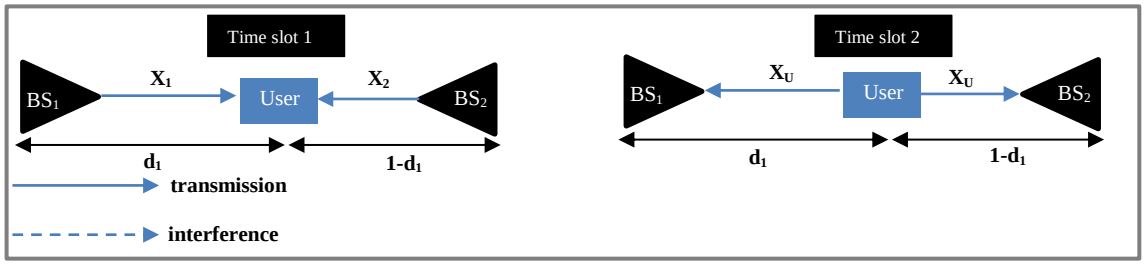

Figure 2. Mode A is illustrated on left side and mode B is illustrated on right side

For our proposed Case 2, the mode A during the first time slot is made up of a downlink transmission from BS_1 to the user and concurrently an uplink transmission from the user to BS_2. The mode B, occurring in the second time slot, on the other hand is made up of the uplink transmission from the user to BS_1 and the downlink transmission from BS_2 to user. Note that when BS_1 (mode A) or BS_2 (mode B) transmit to user, it causes interference to the BS_2 or BS_1, respectively. The key difference of Case 2 from Case 1 is that the user adopts IBFD technique, allowing it to communicate in both directions simultaneously using similar frequency. Figure 3 summarizes the entire transmissions of mode A and mode B for case 2. Here, the received signals for mode A are defined as

$$Y_u = h_{1u}X_1 + N_o \quad (2a)$$

$$Y_2 = h_{u2}X_u + h_{12}X_1 + N_o \quad (2b)$$

and for mode B are defined as

$$Y_u = h_{2u}X_2 + N_o$$

$$Y_1 = h_{u1}X_u + h_{21}X_2 + N_o$$

Figure 4 summarized the transmission schemes of Case 3, where it adopts the OMA concept whereby the bandwidth of β (0 < β< 1) Hz is shared between BS_1 and BS_2 for uplink and downlink transmission mode. In Case 3, there is no interference exists as different frequencies are used at different base stations. The received signals that happens during the first (mode A) and second (mode B) time slots for Case 3 are respectively defined as

$$Y_u^{(fi)} = X_{iu} + N_o \quad (3a)$$

$$Y_i^{(fi)} = X_{ui} + N_o. \quad (3b)$$

We denote superscript f_i, $i \in \{1,2\}$ to define the two orthogonal frequencies used to forward the messages concurrently under OMA scheme.

The final benchmarked schemes are the state-of-the-art point-point communication between the user and base station as shown in Figure 5. Mode A and mode B of the point-to point downlink and uplink transmissions occur using different time slots. We denote the communication between BS_1 and user as Case 4, while the communication between user and BS_2 is referred to as Case 5. The received signals for point-point communication are defined as

$$Y_u = h_{iu}X_i + N_o; \text{ for mode A and } i \in \{1,2\} \quad (4a)$$

$$Y_j = h_{uj}X_u + N_o; \text{ for mode B and } j \in \{1,2\} \quad (4b)$$

where $i, j = 1$ denotes case 4, while case 5 is represented using $i, j = 2$.

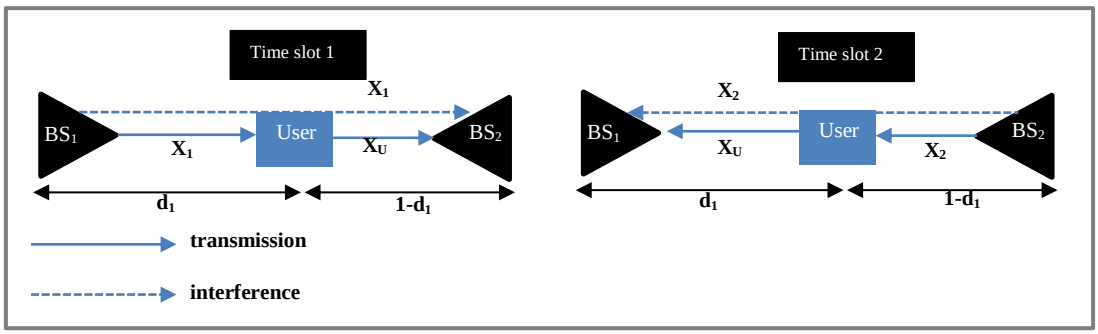

Figure 3. Mode A is shown on left hand side whereby mode B is shown on right hand side

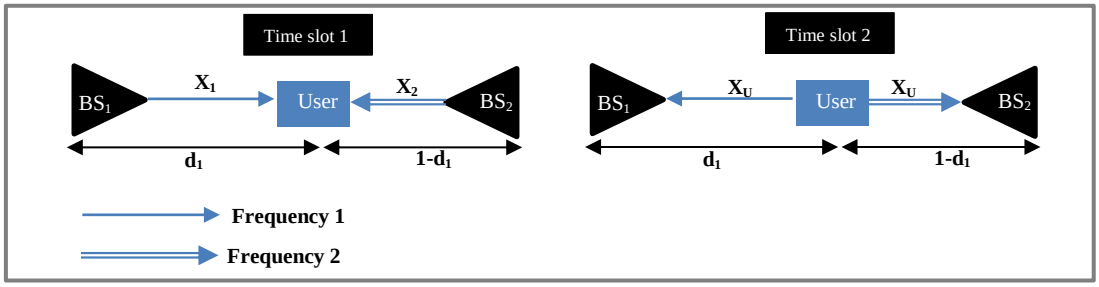

Figure 4. Mode A is illustrated on left hand side whereby Mode B is illustrated on right hand side

Figure 5. Case 4 is illustrated on left hand side whereby Case 5 is illustrated on right hand side

3. Achievable Rates

This section derives the achievable rate for the proposed NOMA schemes and the benchmarked schemes of Orthogonal Multiple Access and Point-to-Point communications to evaluate and analyze their performances.

3.1. NOMA (Case 1 and Case 2)

Successive Interference Cancellation (SIC) is the key physical layer techniques used to concurrently decode two or more signals under NOMA schemes. The first step for the receiver to decode two concurrent signals using SIC is to start with the decoding of messages corresponding to the stronger signals, while treating the weaker signal as an interference. Once this is correctly performed, only then the receiver can cancel out the stronger signals and decode the message corresponding to the weaker signal in the second step. Before we begin the derivation of the achievable rate, let us define the received signal power at node j from node i

$$\mathrm{P_{ij}} = \mathrm{P_i}\,\mathrm{h_{ij}}^2. \tag{5}$$

using (5), the signal-to-interference-noise ratio (SNIR) and signal-to-noise ratio (SNR) parameters at receiver node j, assuming the stronger and weaker signals are transmitted from node s and w, respectively are

$$\mathrm{SNIR_{sj}} = \frac{\mathrm{P_{sj}}}{\mathrm{P_{wj}+N_o}}, \tag{6}$$

$$\mathrm{SNR_{wj}} = \frac{\mathrm{P_{wj}}}{\mathrm{N_o}}. \tag{7}$$

for a normalized bandwidth B=1, the achievable rates at node j for the stronger and weaker channels when adopting SIC techniques are

$$\mathrm{R_s} = \log_2\left(1+\mathrm{SNIR_{sj}}\right) \tag{8}$$

$$\mathrm{R_w} = \log_2\left(1+\mathrm{SNR_{wj}}\right), \tag{9}$$

which gives the total achievable rates at node j when using SIC to be

$$\mathrm{R_{SIC}} = \mathrm{R_s} + \mathrm{R_w} \tag{10}$$

throughout this derivation, we use a normalized bandwidth of 1. Let us now use the concept of SIC to derive the achievable rates for the proposed NOMA schemes of case 1 and case 2. For the conventional NOMA of Case 1 (mode A), the user is receiving signals concurrently from both BSs. Denoting the base stations with stronger and weaker signals using subscript s and w, respectively, the achievable rates of Case 1 (mode A) are (11)

$$\mathrm{R^{(1A)}} = \log_2\left(1+\frac{\mathrm{P_s.h_{su}^2}}{\mathrm{P_w.h_{wu}^2+N_o}}\right) + \log_2\left(1+\frac{\mathrm{P_w.h_{wu}^2}}{\mathrm{N_o}}\right) \tag{11}$$

for $s,w \in \{1,2\}$ and $s \neq w$. During mode B, the user is forwarding the same message to both base stations simultaneously using superimposed power allocation signal that consist of respective message from both base stations. Defining the power allocation at the user as $P_u = P_u^{(1)} + P_u^{(2)}$, where P_u is the total transmit power at user and $P_u^{(j)}$ is the power used to forward messages from user to base station j. Upon receiving the message at BS_1, BS_1 applies SIC technique to remove the interference signal from BS_2 if the certain condition is satisfied. Therefore, the achievable rate at BS_1 can be written as (12)

$$R_{u1}^{(1B)}=\begin{cases}\log_2\left(1+\frac{P_u^{(1)}.h_{u1}^2}{N_o}\right) & if\ \frac{P_u^{(2)}.h_{u1}^2}{P_u^{(1)}.h_{u1}^2+N_o}>\frac{P_u^{(2)}.h_{u2}^2}{N_o},\\ \log_2\left(1+\frac{P_u^{(1)}.h_{u1}^2}{N_o}\right) & if\ \frac{P_u^{(2)}.h_{u1}^2}{P_u^{(1)}.h_{u1}^2+N_o}>\frac{P_u^{(2)}.h_{u2}^2}{N_o}\ \&\ \frac{P_u^{(2)}.h_{u1}^2}{P_u^{(1)}.h_{u1}^2+N_o}>\frac{P_u^{(2)}.h_{u2}^2}{P_u^{(1)}.h_{u2}^2+N_o}\ \&\ \frac{P_u^{(1)}.h_{u2}^2}{P_u^{(2)}.h_{u2}^2+N_o}\le\frac{P_u^{(1)}.h_{u1}^2}{N_o}\ \&\\ & \frac{P_u^{(1)}.h_{u2}^2}{P_u^{(2)}.h_{u2}^2+N_o}\le\frac{P_u^{(1)}.h_{u1}^2}{P_u^{(2)}h_{u1}^2+N_o},\\ \log_2(1+\frac{P_u^{(1)}.h_{u1}^2}{P_u^{(2)}.h_{u1}^2+N_o}) & else\end{cases}\quad(12)$$

as for the BS_2, different conditions are applied in order to implement SIC to remove the interference. As a result, it can only decode at (13).

$$R_{u2}^{(1B)}=\begin{cases}\log_2\left(1+\frac{P_u^{(2)}.h_{u2}^2}{N_o}\right) & \text{if}\ \frac{P_u^{(1)}.h_{u2}^2}{P_u^{(2)}.h_{u2}^2+N_o}>\frac{P_u^{(1)}.h_{u1}^2}{N_o},\\ \log_2\left(1+\frac{P_u^{(2)}.h_{u2}^2}{N_o}\right) & \text{if}\ \frac{P_u^{(2)}.h_{u1}^2}{P_u^{(1)}.h_{u1}^2+N_o}\le\frac{P_u^{(2)}.h_{u2}^2}{N_o}\ \&\ \frac{P_u^{(1)}.h_{u2}^2}{P_u^{(2)}.h_{u2}^2+N_o}\le\frac{P_u^{(1)}.h_{u1}^2}{N_o}\ \&\ \frac{P_u^{(1)}.h_{u2}^2}{P_u^{(2)}.h_{u2}^2+N_o}>\frac{P_u^{(1)}.h_{u1}^2}{P_u^{(2)}h_{u1}^2+N_o},\\ \log_2\left(1+\frac{P_u^{(2)}.h_{u2}^2}{P_u^{(1)}.h_{u1}^2+N_o}\right) & \text{else}\end{cases}\quad(13)$$

The achievable rate for case 1 (mode B) is given by (14).

$$R^{(1B)}=R_{u1}{}^{(1B)}+R_{u2}{}^{(1B)}\quad(14)$$

The total achievable rate for case 1 can be computed by adding the rates during mode A and mode B as follows

$$R_t^{(1)}=R^{(1A)}+R^{(1B)}\quad(15)$$

now, we explain the derivation of the achievable rate for our proposed case 2. Our case 2 NOMA scheme is different from the conventional case 1 NOMA, whereby user during mode A or B receives its intended messages without any interference. As a result, the achievable rates at the user during mode A and B can be written, respectively, as

$$R_{1u}{}^{(2A)}=\log_2\left(1+\frac{P_1.h_{1u}^2}{N_o}\right)\quad(16)$$

$$R_{2u}{}^{(2B)}=\log_2\left(1+\frac{P_2.h_{2u}^2}{N_o}\right)\quad(17)$$

as for the detection of signals at the base stations, from (2b), BS_2 during mode A needs to decode the message from the user while at the same time it also receives an interference signal from BS_1. Here BS_2 can only apply SIC technique to remove the interference signal from BS_1 if the following condition is satisfied

$$R_{u2}^{(2A)}=\begin{cases}\log_2\left(1+\frac{P_u.h_{u2}^2}{N_o}\right) & \text{if}\ \frac{P_1.h_{12}^2}{P_u.h_{u2}^2+N_o}\ge\frac{P_1.h_{1u}^2}{N_o}\\ \log_2\left(1+\frac{P_u.h_{u2}^2}{P_1.h_{12}^2+N_o}\right) & \text{else}\end{cases}\quad(19)$$

using similar approach and condition when obtaining the achievable rate of (19), the achievable rate at BS_1 during mode B is given by (20).

$$R_{u1}^{(2B)}=\begin{cases}\log_2\left(1+\frac{P_u.h_{u1}^2}{N_o}\right) & \text{if}\ \frac{P_2.h_{21}^2}{P_u.h_{u1}^2+N_o}\ge\frac{P_2.h_{2u}^2}{N_o}\\ \log_2\left(1+\frac{P_u.h_{u1}^2}{P_2.h_{21}^2+N_o}\right) & \text{else}\end{cases}\quad(20)$$

The total rate during mode A and mode B, respectively, for case 2 can be summarized as

$$R^{(2A)} = {R_{1u}}^{(2A)} + {R_{u2}}^{(2A)} \quad (21)$$

$$R^{(2B)} = {R_{2u}}^{(2B)} + {R_{u1}}^{(2B)} \quad (22)$$

finally, the total achievable rate for case 2 can be written as

$$R_t^{(2)} = R^{(2A)} + R^{(2B)} \quad (23)$$

3.2. Benchmarked Scheme

For comparison purposes, we also provide the achievable rates for the following two benchmark schemes. First benchmarked scheme is named Case 3 that adopts the OMA transmission schemes, whereby the bandwidth of B Hz is shared between BS_1 and BS_2 in respective uplink and downlink transmission mode. On the other hand, for Case 4 and Case 5, each of the case comprises of point-to-point transmission between User and BS_1 or BS_2 respectively.

3.2.1. OMA (Case 3)

Case 3 adopts OMA schemes with θ bandwith allocation assigned for BS_1 to user channel and (1-θ) bandwith allocation for BS2 to user channel during the respective downlink (i.e. Case 3A) and uplink (i.e. Case 3B) transmissions. The achievable rates for downlink and uplink transmission of OMA are defined respectively as (24) and (25).

$$R^{(3A)} = {R_{1u}}^{(3A)} + {R_{2u}}^{(3A)} = \theta \log_2\left(1 + \frac{P_1.h_{1u}^2}{N_o}\right) + (1-\theta)\log_2\left(1 + \frac{P_2.h_{2u}^2}{N_o}\right) \quad (24)$$

$$R^{(3B)} = {R_{u1}}^{(3B)} + {R_{u2}}^{(3B)} = \theta \log_2\left(1 + \frac{P_u.h_{u1}^2}{N_o}\right) + (1-\theta)\log_2\left(1 + \frac{P_u.h_{u2}^2}{N_o}\right) \quad (25)$$

The total achievable rate of OMA schemes is (26).

$$R^{(3)} = R^{(3A)} + R^{(3B)} \quad (26)$$

3.2.2. Point-to-point transmissions (Case 4 and Case 5)

Cases 4 and 5 are two conventional point-to-point transmission schemes for the user to BS_1 and user to BS_2 links, respectively. The total achievable rate of cases 4 and 5, respectively, are:

$$R^{(4)} = {R_{u1}}^{(4A)} + {R_{1u}}^{(4B)} = \log_2\left(1 + \frac{P_u.h_{u1}^2}{N_o}\right) + \log_2\left(1 + \frac{P_1.h_{1u}^2}{N_o}\right) \quad (27)$$

$$R^{(5)} = {R_{u2}}^{(5A)} + {R_{2u}}^{(5B)} = \log_2\left(1 + \frac{P_u.h_{u2}^2}{N_o}\right) + \log_2\left(1 + \frac{P_2.h_{2u}^2}{N_o}\right) \quad (28)$$

4. Numerical Result

This section presents the analytical results comparing our proposed schemes (case 2) with the conventional NOMA schme (case 1) and benchmarked schemes (case 3, 4 and 5). We set the transmission power for each mode A and B to 1, and plot the achievable rates of all five cases against the 9 locations of user from BS_1, i.e. d_1 = {0.1, 0.2, 0.3, 0.4, 0.5, 0.6, 0.7, 0.8, 0.9}. For case 1 and 2, all nodes are allocated Pi=0.5, for i∈{1,2,u}, except for the power allocated to the user during mode B of case 1, where $P_u = {P_u}^{(1)} + {P_u}^{(2)} = 1$. For case 1 (mode B), depending on strength of the channel gain, we allocate a power allocation of 0.9 to the stronger link. This is to ensure that the weaker channel is still active with a power of 0.1. Note that, using a different power allocation provides different rates for case 1. As for case 3, 4, and 5, all nodes are allocated Pi=1, for i∈{1,2,u} } to maintain the normalized power of 1 in each mode. Setting all transmitted powers in such a way ensure each case to be fairly compared with a total transmitted power of 2 for both mode A and B.

Figure 6 presents the achievable rates of mode A in case 1, $R^{(1A)}$, case 2, $R_{1u}^{(2A)} + R_{2u}^{(2B)}$, case 3, $R^{(3A)}$, case 4, $R^{(4A)}$ and case 5, $R^{(5A)}$. We can see our proposed scheme (case 2), IBFD technique under NOMA scheme attains the highest achievable rates among the 5 cases in mode A. From Figure 6, it shows that our proposed scheme successfully improves 64 percent based on $R_{1u}^{(2A)} + R_{2u}^{(2B)}$, 8.934 bps/Hz compare with other schemes that attaining the same achievable rate, 5.434 bps/Hz when located at $d_1 = 0.5$. Furthermore, it is suspected that d_1=0.5 is the cell edge of both BSs due to the symmetry U shape for the user centric NOMA and OMA schemes obtain the lowest achievable rate at d_1=0.5. At point-to point concept, the user gains higher achievable when his location is close to BS_1(d_2=0). However due to the reception signal is getting faded when he is getting away from BS1, the achievable rate reaches the lowest when it reaches d_1=1.0.

Figure 7 presents the achievable rates of mode B in case 1, $R^{(1B)}$, case 2, $R_{u2}^{(2A)} + R_{u1}^{(2B)}$, case 3, $R^{(3B)}$, case 4, $R^{(4B)}$ and case 5, $R^{(5B)}$. We can see that at uplink transmission, all cases remain the same shape with symmetry U shape for the user centric NOMA and OMA schemes. Besides that, Figure 7 also shows that the achievable rate stays the same in both downlink and uplink obtained by OMA Case 3, point-to point case 4 and case 5 as mentioned that its reciprocal relationship with its downlink transmission. From Figure 7, the conventional NOMA case 1 has lowest rate, 3.197 bps/Hz compared to other schemes, 5.434bps/Hz at d1=0.5 except for case 2. The reason being is both base stations are allocated with the 0.9 and 0.1 power allocations to ensure the base station with weaker channels can only decode its signal by treating the signals to the stronger base station as interference. As a result, we notice that it is better to adopt OMA and point-to point scheme than NOMA case 1 especially at low point location, d_1=0.5. Again, Figure 7 shows that our proposed scheme successfully improves 44 percent based on $R_{u2}^{(2A)} + R_{u1}^{(2B)}$, 7.828 bps/Hz compare with other schemes that attaining the same achievable rate, 5.434 bps/Hz at $d_1 = 0.5$.

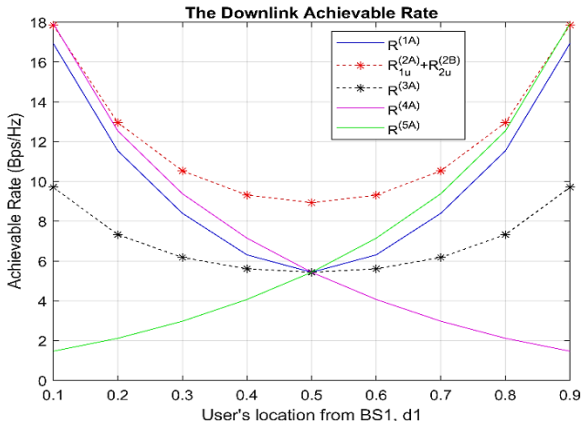

Figure 6. The achievable rates in downlink transmission

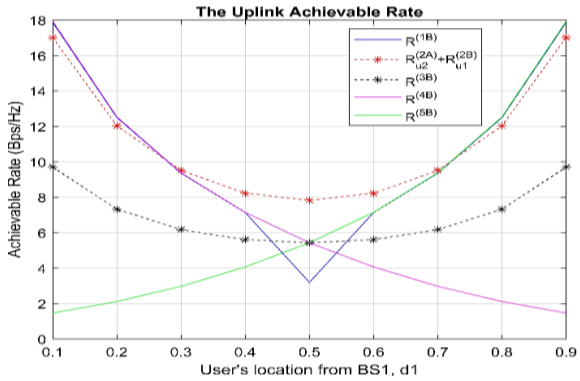

Figure 7. The achievable rates in uplink transmission

Finally, Figure 8 presents the total achievable rates of $R^{(1)}$, $R^{(2)}$,$R^{(3)}$,$R^{(4)}$ and $R^{(5)}$ for every case 1, 2, 3, 4 and 5, respectively. We can see that NOMA with IBFD user improves the performance at about 54 percentage when compared to OMA, hand-off point-to-point communication at d_1=0.5. This indicates the superiority of our proposed case 2 specially to improve the achievable rates at the cell boundries.

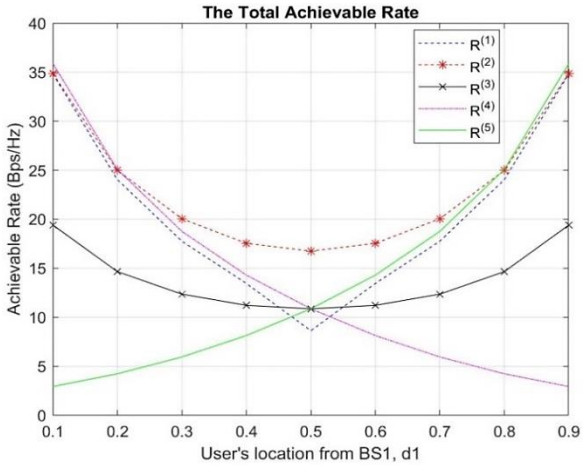

Figure 8. The total achievable rates

5. Conclusion

Through this research work, we have shown that our proposed scheme at case 2 excels in the achievable rate compare with the conventional NOMA scheme and other benchmarked schemes under similar power constraint in mode A and mode B. From the angle of spectral efficiency, our proposed scheme has successfully offered frequency sharing among the users and BS while attaining good achievable rates for both uplink and downlink along the distance. Although point- to-point communication leads ahead when they placed near to the BS but this is not practical for our future resource allocation with the explosive growth of the data traffic. The insights obtained from this initial study will be enhanced to the future works.

Acknowledgements

Authors would like to express utmost gratitude to the Ministry of Education (MOE) in Malaysia and Universiti Teknologi Malaysia (UTM) for providing finiancial support for this research through HiCOE grant(R.J130000.7823.4J215). The grant is managed by Research Management Centre (RMC) at UTM.

References

[1] Sabharwal A, Schniter P, Guo D, Bliss DW, Rangarajan S, Wichman R. In-Band Full-Duplex Wireless: Challenges and Opportunities. *IEEE Journal on Selected Areas in Communications.* 2014; 32(9): 1637-1652.
[2] Goyal S, Liu P, Hua S, Panwar S. *Analyzing a Full-Duplex Cellular System*. 47th Annual Conference on Information Sciences and Systems. 2013: 20-22.
[3] Andrews JG, Buzzi S, et al. What Will 5G Be?. *IEEE Journal on Selected Areas in Communications*. 2014; 32(6): 1065-1082.
[4] Tse D, Viswanath P. Fundamentals of Wireless Communication. Cambridge University Press. 2005: 166-217.
[5] Caire G, Shamai S. On The Achievable Throughput of a Multi-Antenna Gaussian Broadcast Channel. *IEEE Trans. Info. Theory*. 2003; 49(7): 1692–1706.
[6] Higuchi K, Kishiyama Y. Non-Orthogonal Access with Successive Interference Cancellation for Future Radio Access. *IEICE TRANS.Commun*. 2015; E98-B: 403-414.

[7] Endo Y, Kishiyama Y, Higuchi K. *Uplink Non-Orthogonal Access with MMSE-SIC In The Presence of Intercell Interference*. International Symposium on Wireless Communication Systems. 2012: 261–265.
[8] Benjebbour A, Saito Y, Kishiyama Y, Li A, Harada A, Nakamura T. *Concept and Practical Considerations of Non-Orthogonal Multiple Access (NOMA) For Future Radio Access*. Proc. IEEE ISPACS. 2013: 770–774.
[9] Saito Y, Benjebbour A, Kishiyama Y, Nakamura T. *System-Level Performance Evaluation Of Downlink Non-Orthogonal Multiple Access (NOMA)*. Proc. IEEE PIMRC 2013. 2013: 611–615.
[10] Benjebbovu A, Li A, Saito Y, Kishiyama Y, Harada A, Nakamura T. *System-Level Performance Of Downlink NOMA for Future LTE Enhancements*. IEEE Globecom. 2013: 66–70.
[11] Higuchi K, Kishiyama Y. *Non-Orthogonal Access with Random Beamforming and Intra-Beam SIC For Cellular MIMO Downlink*. Proc. IEEE VTC2013-Fall. 2013: 1–5.
[12] Li A, Benjebbour A, Harada A. *Benjebbour and A.Harada. Performance Evaluation Of Non-Orthogonal Multiple Access Combined With Opportunistic Beamforming*. Proc. IEEE VTC Spring 2014. Seoul. 2014: 1-5.
[13] Choi J. Non-Orthogonal Multiple Access In Downlink Coordinated Two Point Systems. *IEEE Communication Letters.* 2014; 18(2): 313-316.
[14] Beylerian A, Ohtsuki T. *Coordinated NOMA (CO-NOMA)*. IEEE Global Communications Conference (GLOBECOM). Washington. 2016: 1-5.
[15] Dai L, Wang B, Yuan Y, Han S, Chih-Lin I, Wang Z. Non-Orthogonal Multiple Access for 5G: Solutions, Challenges, Opportunities, and Future Research Trends. *IEEE Communications Magazine*. 2015; 53(9): 74-81.
[16] Song L, Li Y, Ding Z, Poor HV. Resource Management in Non-Orthogonal Multiple Access Networks for 5G and Beyond. *IEEE Network*. 2017; 33: 8-14.
[17] Saito Y, Kishiyama Y, Benjebbour A, Nakamura T, Li A, Higuchi K. *Non-Orthogonal Multiple Access (NOMA) for Cellular Future Radio Access*. IEEE 77th Vehicular Technology Conference (VTC Spring). Dresden. 2013: 1-5.
[18] Wunder G, Kasparick M, et al. *System-Level Interfaces And Performance Evaluation Methodology for 5G Physical Layer Based On Non-Orthogonal Waveforms*. Asilomar Conference on Signals, Systems and Computers. Pacific Grove. 2013: 1659-163.
[19] Han T, Gong J, et al. On Downlink NOMA in Heterogeneous Networks with Non-Uniform Small Cell Deployment. *IEEE Access*. 2018; 6: 31099–31109.
[20] Choi J. Non-Orthogonal Multiple Access in Downlink Coordinated Two-Point Systems. *IEEE Communications Letters*. 2014; 18(2): 313-316.
[21] Thomsen H, Popovski P, et al. CoMPflex: CoMP for In-Band Wireless Full Duplex. *IEEE Wireless Communications Letters*. 2016; 5(2): 144-147.
[22] Guy Daniels. [Updated] SK Telecom and Ericsson Demonstrate 5G Elastic Cell Technology. Telecom TV: 5G. 21 July 2014.
[23] Zhang H, Meng N, Liu Y, Zhang X. Performance Evaluation for Local Anchor-Based Dual Connectivity in 5G User-Centric Network. *IEEE Access*. 2016; 4: 5721-5729.
[24] Pan C, Elkashlan M, Wang J, Yuan J, Hanzo L. User-Centric C-RAN Architecture for Ultra-Dense 5G Networks: Challenges and Methodologies. *IEEE Communications Magazine*. 2018; 56(6): 14-20.
[25] Liu Y, Li X, Yu FR, Ji H, Zhang H, Leung VC. Grouping and Cooperating among Access Points in User-Centric Ultra Dense Networks with Non-Orthogonal Multiple Access. *IEEE Journal on Selected Areas in Communications*. 2017; 35(10): 2295-2311.